

## A Novel Low-Dimensional Method for Analytically Solving Partial Differential Equations

Jie Sha<sup>1</sup>, Lixiang Zhang<sup>1</sup> and Chuijie Wu<sup>2,\*</sup>

<sup>1</sup> Department of Engineering Mechanics, Kunming University of Science and Technology, Kunming 650500, Yunnan, China

<sup>2</sup> State Key Laboratory of Structural Analysis for Industrial Equipment School of Aeronautics and Astronautics, Dalian University of Technology, Dalian 116024, China

Received 24 June 2014; Accepted (in revised version) 14 November 2014

---

**Abstract.** This paper is concerned with a low-dimensional dynamical system model for analytically solving partial differential equations (PDEs). The model proposed is based on a posterior optimal truncated weighted residue (POT-WR) method, by which an infinite dimensional PDE is optimally truncated and analytically solved in required condition of accuracy. To end that, a POT-WR condition for PDE under consideration is used as a dynamically optimal control criterion with the solving process. A set of bases needs to be constructed without any reference database in order to establish a space to describe low-dimensional dynamical system that is required. The Lagrangian multiplier is introduced to release the constraints due to the Galerkin projection, and a penalty function is also employed to remove the orthogonal constraints. According to the extreme principle, a set of ordinary differential equations is thus obtained by taking the variational operation of the generalized optimal function. A conjugate gradient algorithm by FORTRAN code is developed to solve the ordinary differential equations. The two examples of one-dimensional heat transfer equation and nonlinear Burgers' equation show that the analytical results on the method proposed are good agreement with the numerical simulations and analytical solutions in references, and the dominant characteristics of the dynamics are well captured in case of few bases used only.

**AMS subject classifications:** 65M10, 78A48

**Key words:** Low-dimensional system model, partial differential equation, analytical solution, posterior optimal truncated method.

---

### 1 Introduction

Over the past few decades, scientists and engineers were considerable interest in looking for an order-reduced method to effectively model partial differential equations (PDEs).

---

\*Corresponding author.

Email: shajie9981@gmail.com (J. Sha), zlxzcc@126.com (L. X. Zhang), cjwudut@dlut.edu.cn (C. J. Wu)

One of the crucial study motivations is to seek a way to analytically solve reduction order models of a high dimensionality system, while it is generally solved by using a mesh-based discretization technique to investigate the constitutive equation of a physical problem. An analytical solution for a linear low-dimensional problem is ever expected. Unfortunately, the expectation seems to be impossible to most high-dimensional systems, because the nonlinear systems such as high-dimensionality may have quite complex dynamical behaviors, ever possibly evolve into chaos. Therefore, it is extremely valuable if a reduction dimensionality method can be built well to analytically analyze high order dynamical systems.

At the present stage, there are several analytical methods well developed based on the *posterior* and *prior* reduction dimensionality techniques, respectively. Locally linear embedding (LLE) [1] method approximates the local geometry by linear coefficients that are used to reconstruct data points in neighbors, in which the reconstruction errors are controlled by the squared distances between reconstruction data points. The crux of ISOMAP [2] preserves the geodesic manifold distances between all pairs of the data points. As a powerful tool, the proper orthogonal decomposition (POD), firstly introduced by Lumley for studying long-term behavior of turbulence, is beyond reasonable doubt an outstanding *posterior* reduced method. A set of bases is obtained by using POD with a database of experiments or numerical simulations, and these bases on POD are mathematically proved to be optimum in terms of energy. Other attractive property of POD is linear processing while minimizing the average squared distance between the original configuration space and the reduced linear one. Consequently, POD become quite useful to reduce order of a system by construction of new bases on the information under investigative objects [3–6]. Also, POD is valuable to be used by conjunction with other techniques [7–9], for example, Galerkin projection method, to well predict complex dynamics of an airfoil induced by unsteady transonic flow. On the other hand, POD is developed as an order-reduced model with multiple parameters [10,11], by which unstable phenomenon [12] in numerical simulation is effectively suppressed, and computing algorithm is more efficient [13–16]. However, it is noted that a notable shortcoming of the POD methods is highly dependent on *prior* data to construct optimal bases. Thus, the enormous computational cost of numerical simulation, and the time-consuming work of experiment, as well as obtaining usable *prior* data become a challenge in application. So, it is quite necessary to look for a way to circumvent the drawbacks of the *posterior* methods.

Approaching on truncated series expansion is expected to be a good way to overcome the shortcoming of the *posterior* methods, for example, the order-reduced methods on Laguerre polynomials [17]. The methods on other orthonormal polynomials, such as Fourier polynomials, are universal, but it is hard to mathematically deal with boundary conditions. In order to solve the problems of boundary conditions, scientists develop measure methodologies, for example, the proper generalized decomposition (PGD) proposed by Ammar, which is able to well treat multidimensional problems. PGD separates variables by defining a tensor product of unknown approximation basis, and then car-

ries out an iteration procedure of three steps, which projects the solution onto a discrete basis, and checks convergence and enrichment of the approximation basis, respectively [18, 19]. A suitable iterative scheme is required to solve the nonlinear or linear system which is decomposed with trial and test functions by projection methods. Furthermore, the finite element method is widely used to solve the weak form of the system, or the finite difference method for the strong form [20]. A quasi-residual term is taken as the convergence criterion for iteration scheme. Recently, PGD has been well used to deal with various scientific problems and made advancements for different physical models in high dimensions.

With a relationship between coherent structures and low-dimensional dynamical systems (LLDS), Wu and Shi proposed a new method, named the optimal truncated(OT) LDDS. LDDS OT is a *posterior* or *prior* dimensional reduced method whether a given database is used or not [21]. The system under consideration is decomposed with a finite term sum of time-dependent modal coefficients multiplied by spatial bases functions to be determined. LDDS is obtained as a constraint condition on the optimal control is processed by Galerkin projection of PDE onto the unknown spatial bases. Therefore, a set of orthogonal spatial bases is found out by solving an extremely valued problem with the constraint of LDDS. If LDDS is constructed on a given database, the corresponding method is called as *prior* DOT (Database OT), otherwise, as *posterior* POT (PDE OT). These methods can effectively reduce the dimensions of the system under consideration. But, the error control is not well dealt with when the residue is taken as an objective of the global optimization. It means that the error may dramatically rise and the optimization solution fails.

In the present paper, a new optimal control criterion is proposed to solve the problem in reference [21]. The paper is outlined as follow. Firstly, the fundamentals and establishments of the method proposed are described with details, Then, solutions of the linear and nonlinear PDEs are taken as examples to validate the proposed method by comparisons with the results from references. Finally, a summary of the study is arranged as conclusion.

## 2 Formulations

Considering a well-posed operator equation is as follow,

$$\begin{cases} \frac{\partial \vec{u}}{\partial t} + L(\vec{u}) = 0, & \vec{x} \in \Omega, \quad t > 0, \\ \vec{u}(\vec{x}, 0) = \vec{u}_0(\vec{x}), & \vec{x} \in \Omega, \\ \vec{u}(\vec{x}, t)|_{\partial\Omega} = \vec{g}(\vec{x}, t), & \vec{x} \in \partial\Omega, \quad t > 0. \end{cases} \quad (2.1)$$

Where, for all  $t > 0$ ,  $L: \mathcal{H} \subset \mathcal{V} \rightarrow \mathcal{F}$  is a linear or nonlinear operator,  $\mathcal{H}$ ,  $\mathcal{V}$  and  $\mathcal{F}$  are the Hilbert spaces.  $\mathcal{H}$  is the linear subspace of  $\mathcal{V}$ . The inner products on  $\mathcal{H}$ ,  $\mathcal{V}$  and  $\mathcal{F}$  are

represented by  $(\cdot, \cdot)_{\mathcal{H}}$ ,  $(\cdot, \cdot)_{\mathcal{V}}$  and  $(\cdot, \cdot)_{\mathcal{F}}$ , respectively. The corresponding norms on  $\mathcal{V}$  are defined as  $\|\vec{u}\|_2 = (\vec{u}, \vec{u})_{\mathcal{V}}^{1/2}$  and  $\|(\vec{u}, \vec{v})\|_1 = (\vec{u}, \vec{v})_{\mathcal{V}}$  for all  $\vec{u}, \vec{v} \in \mathcal{V}$

Since a space-time separation is applied to the variables, the spatial function of each time  $t$  belongs to an appropriate space,  $\mathfrak{R}$ , defined over the domain  $\Omega$ , and written as

$$\mathfrak{R} \triangleq \left\{ \vec{\zeta} = (\vec{\zeta}_1(\vec{x}), \dots, \vec{\zeta}_{N_t}(\vec{x}))^T \mid \vec{\zeta}_i \in \mathcal{H}, \vec{\zeta}_i|_{\partial\Omega} = 0, (\vec{\zeta}_i, \vec{\zeta}_j) = \delta_{ij} \right\}. \quad (2.2)$$

It is noted that the boundary conditions of the operator function are included in Eq. (2.2), and the orthogonal conditions are satisfied. Decomposing variables in equation as a finite term sum of time-dependent modal coefficients multiplied by elements of a suitable basis of  $\mathfrak{R}$ , it yields

$$\vec{u}(\vec{x}, t) = \vec{u}_{N_t} + \vec{u}_R \approx \sum_{k=1}^{N_t} a_k(t) \vec{\zeta}_k(\vec{x}), \quad (2.3)$$

where, the coefficient  $a_k$  is subjected to the Galerkin projection of the equation which is constructed by projecting Eq. (2.1) onto the unknown basis  $\vec{\zeta}_l$ , and  $G_l$  denotes the projecting equation as follow:

$$\begin{cases} G_l = F(a_l; \dot{a}_l; \vec{\zeta}_1, \dots, \vec{\zeta}_{N_t}; \nabla \vec{\zeta}_1, \dots, \nabla \vec{\zeta}_{N_t}, \dots), \\ a_l(0) = (\vec{u}_0(\vec{x}), \vec{\zeta}_l), \end{cases} \quad (2.4)$$

where,  $l = 1, 2, 3, \dots, N_t$ . The specific form of Eq. (2.4) depends on the problem under investigation.

In order to make the remainder  $\|\vec{u}_R\|$  approach to zero, and to construct an authentic LDDS, a control function  $J(\vec{\zeta})$  is built as follow,

$$\begin{aligned} J(\vec{\zeta}) = & \mu_1 \int_0^T \|\vec{u}_R\|_2^2 dt + \mu_2 \|\vec{u}_0(\vec{x}) - \sum_{k=1}^{N_t} a_k(0) \vec{\zeta}_k(\vec{x})\|_2^2 \\ & + \mu_3 \int_0^T \left\| \frac{\partial \vec{u}_{N_t}}{\partial t} + L(\vec{u}_{N_t}) \right\|_2^2 + \mu_4 \int_0^T \left\| \left( \frac{\partial \vec{u}_{N_t}}{\partial t} + L(\vec{u}_{N_t}), \vec{\zeta}_l \right) \right\|_1 dt, \end{aligned} \quad (2.5)$$

where,  $\mu_i$  ( $i = 1, 2, 3, 4$ ) is the weighted coefficient. The optimal control search is described as follow,

$$\text{Find } \vec{\zeta}^* \in \mathfrak{R}, \text{ such that } J(\vec{\zeta}^*) = \min_{\vec{\zeta} \in \mathfrak{R}} J(\vec{\zeta}), \text{ where } a_l \text{ satisfies Eq. (2.5)}. \quad (2.6)$$

The first three terms at the right hand side of Eq. (2.5) were studied by Wu and his colleagues. For the DOT method,  $\vec{u}$  is a given data. Thus,  $\vec{u}_R$  is determined once  $\vec{u}_{N_t}$  is set. Hence, the control function has a form as follow,

$$J(\vec{\zeta}) = \mu_1 \int_0^T \|\vec{u}_R\|_2^2 dt + \mu_2 \left\| \vec{u}_0(\vec{x}) - \sum_{k=1}^{N_t} a_k(0) \vec{\zeta}_k(\vec{x}) \right\|_2^2 + \mu_3 \int_0^T \left\| \frac{\partial \vec{u}_{N_t}}{\partial t} + L(\vec{u}_{N_t}) \right\|_2^2. \quad (2.7)$$

However,  $\vec{u}$  is unknown for the POT method. Consequently,  $\vec{u}_R$  is unknown as well. It is noted that the first and the second terms at the right hand side of Eq. (2.5) can be simplified if some conditions are subjected to it. To do that and to minimize the error of the global "energy" of the system, the first term is written as,

$$\begin{aligned} J(\vec{\xi}) &= \mu_1 \int_0^T \|\vec{u}_R\|_2^2 dt = \mu_1 \int_0^T (\vec{u}_R, \vec{u}_R) dt \\ &= \mu_1 \int_0^T (\vec{u} - \vec{u}_{N_t}, \vec{u} - \vec{u}_{N_t}) dt = \mu_1 \int_0^T [(\vec{u}, \vec{u}) - (\vec{u}_{N_t}, \vec{u}_{N_t}) - 2(\vec{u}_R, \vec{u}_{N_t})] dt, \end{aligned} \quad (2.8)$$

where the integration of  $\int_0^T 2(\vec{u}_R, \vec{u}_{N_t}) dt$  is omitted if assuming that  $\vec{u}_R$  is very small. But, the value of  $\vec{u}_R$  is generally not estimated in advance. So, it takes risk of omitting  $\int_0^T 2(\vec{u}_R, \vec{u}_{N_t}) dt$  without guarantee that  $\vec{u}_R$  is small enough. Therefore, Wu took the second term at the right hand side of Eq. (2.5) as a compensation for omitting  $\int_0^T 2(\vec{u}_R, \vec{u}_{N_t}) dt$

$$\begin{aligned} J(\vec{\xi}) &= \mu_2 \left\| \vec{u}_0(\vec{x}) - \sum_{k=1}^{N_t} a_k(0) \vec{\xi}_k(\vec{x}) \right\|_2^2 \\ &= \mu_2 \left( \vec{u}_0(\vec{x}) - \sum_{k=1}^{N_t} a_k(0) \vec{\xi}_k(\vec{x}), \vec{u}_0(\vec{x}) - \sum_{k=1}^{N_t} a_k(0) \vec{\xi}_k(\vec{x}) \right) \\ &= \mu_2 \left[ (\vec{u}_0(\vec{x}), \vec{u}_0(\vec{x})) + \left( \sum_{k=1}^{N_t} a_k(0) \vec{\xi}_k(\vec{x}), \sum_{l=1}^{N_t} a_l(0) \vec{\xi}_l(\vec{x}) \right) - 2 \left( \vec{u}_0(\vec{x}), \sum_{k=1}^{N_t} a_k(0) \vec{\xi}_k(\vec{x}) \right) \right]. \end{aligned} \quad (2.9)$$

Taking account of the orthogonal property of  $\vec{\xi}_k$  in Eq. (2.8) and Eq. (2.9), and  $\int_0^T (\vec{u}, \vec{u}) dt$  and  $(\vec{u}_0(\vec{x}), \vec{u}_0(\vec{x}))$  are constant for a specific system, hence they can be omitted among optimization process. Therefore, Eq. (2.5) is simplified as follow,

$$J(\vec{\xi}) = \mu_3 \int_0^T \left\| \frac{\partial \vec{u}_{N_t}}{\partial t} + L(\vec{u}_{N_t}) \right\|_2^2 dt - \mu_2 \sum_{k=1}^{N_t} a_k^2(0) - \mu_1 \int_0^T \sum_{k=1}^{N_t} a_k^2(t) dt. \quad (2.10)$$

However, it is noted that summation of the first two terms of Eq. (2.7) is not global energy of the system. LDDS based on the corresponding basis fails to show long-term behaviors of the system because the compensation term introduces the initial information. For improvement, the first term of Eq. (2.10) is only taken as the control function, by which the error of the system under the condition of minimizing the residue of the system is investigated. Unfortunately, as mentioned in the above, the error of the system is still out of the control when the residue is taken as the convergent criterion. It means that LDDS based on the corresponding basis is not optimal; on the contrary it could become worse. To solve this problem, a novel optimal functional condition is proposed. The forth term at the right hand side of Eq. (2.5) is the solution that put forward to improve the OT method. The new optimal functional condition on weighted residue is a kind of the POT methods. It is referred to the POT-WR method in this paper.

The optimal function conditions are subjected to the orthogonal constraints of the basis and the Galerkin projection of Eq. (2.4). In variational process, the Lagrangian multiplier is introduced to release the constraints due to the Galerkin projection, and the penalty function is used to remove the orthogonal constraints. Then, a generalized optimal function is constructed as follow,

$$\begin{aligned}
 J(\vec{\zeta}) = & \mu_1 \int_0^T \|\vec{u}_R\|_2^2 dt + \mu_2 \left\| \vec{u}_0(\vec{x}) - \sum_{k=1}^{N_t} a_k(0) \vec{\zeta}_k(\vec{x}) \right\|_2^2 + \mu_3 \int_0^T \left\| \frac{\partial \vec{u}_{N_t}}{\partial t} + L(\vec{u}_{N_t}) \right\|_2^2 \\
 & + \mu_4 \int_0^T \left\| \left( \frac{\partial \vec{u}_{N_t}}{\partial t} + L(\vec{u}_{N_t}), \vec{\zeta}_l \right) \right\|_1 dt + \int_0^T \sum_{l=1}^{N_t} \lambda_l G_l + \mu \sum_{k,l=1, k \leq l}^{N_t} [(\vec{\zeta}_k, \vec{\zeta}_l) - \delta_{kl}]^2. \quad (2.11)
 \end{aligned}$$

By the variational operation of Eq. (2.11), a set of the ordinary differential equations is obtained

$$\begin{cases} \dot{a}_k = f(a_k, \zeta_1, \dots, \zeta_{N_t}, \zeta'_1, \dots, \zeta'_{N_t}, \dots), \\ \dot{\lambda}_k = y(\lambda_k, a_k, \zeta_1, \dots, \zeta_{N_t}, \zeta'_1, \dots, \zeta'_{N_t}, \dots), \\ \nabla J^s = \frac{\partial H}{\partial \vec{\zeta}_k}, \end{cases} \quad (2.12)$$

where,  $H$  is the Hamiltonian function, which is defined as follow,

$$H = L(a_k, \vec{\zeta}_k, \vec{\zeta}'_k, t) + \lambda_l G_l, \quad k, l = 1, 2, \dots, N_t. \quad (2.13)$$

in which  $L$  is the specified control function.

### 3 Examples

In order to verify the POT-WR method proposed by the present paper, one-dimensional heat transfer and nonlinear Burgers' equations are taken as examples with Fourier, Legendre, and Chebyshev polynomials, respectively.

#### 3.1 Algorithm

A FORTRAN code on the conjugate gradient algorithm is compiled and carried out to solve the set of the ordinary differential equations obtained by the variational operation of Eq. (2.11). The solving scheme is as follow,

- Step 1 Initialing the bases  $\vec{\zeta}^{(0)}$ , and specifying maximum iteration number  $i_{max}$ , penalty  $\mu^{(0)}$ , and accuracy requirement  $\varepsilon$ ;
- Step 2 For  $i = 0$ , with the  $\vec{\zeta}^{(i)}$ , integrating the ordinary partial differential equations of  $a_k$  to obtain  $a_k^{(i)}$ ; and reversal integrating the ordinary partial differential equations of  $\lambda_k$  to obtain  $\lambda_k^{(i)}$ ;

Step 3 Calculating the generalized optimal functional gradient  $\nabla J^g$ , which is defined as

$$J^g(\zeta^* + \delta\zeta) - J^g(\zeta^*) \triangleq \int_{\Omega} \nabla J^g \delta\zeta dx + o(\|\delta\zeta\|);$$

and letting  $g^{(i)}(\zeta) = h^{(i)}(\zeta) = -\nabla J^g$ , if  $g^{(i)}(\zeta) = 0$ , and then go to Step 7;

Step 4 Carrying out the one dimensional search to find  $\rho^{(i)} > 0$ , such that

$$J^g(\zeta^{(i)} + \rho^{(i)}h^{(i)}) = \min_{\rho} [J^g(\zeta^{(i)} + \rho^{(i)}h^{(i)}) | \rho > 0];$$

Step 5 Letting  $\tilde{\zeta} = \zeta^{(i)} + \rho^{(i)}h^{(i)}$ ;

Step 6 Executing Step 2 and Step 3 to get  $\nabla \tilde{J}^g$ ;

Step 7 If  $\nabla \tilde{J}^g = 0$ , and the accuracy  $\varepsilon$  is satisfied, the results are obtained and stop the program. Otherwise, letting  $\mu^{(i+1)} = 20 * \mu^{(i)}$ , and go to Step 3 and let

$$g^{(i+1)} = -\nabla \tilde{J}^g, \quad h^{(i+1)} = g^{(i+1)} + \beta_i h^{(i)}, \quad \beta_i = \frac{(g^{(i+1)} - g^{(i)}, g^{(i+1)})}{\|g^{(i)}\|^2};$$

Step 8 If  $i > i_{\max}$ , a failing solution, and stop operating; Otherwise, letting  $i = i + 1$ ,  $\zeta^{(i+1)} = \tilde{\zeta}$  and go to Step 6.

### 3.2 Solving one-dimensional heat transfer equation

The governing equation of one-dimensional heat transfer problem with boundary and initial conditions is written as,

$$\begin{cases} \frac{\partial u}{\partial t} = \varepsilon \frac{\partial^2 u}{\partial x^2}, & t > 0, \quad 0 < x < 1, \\ u(0, t) = u(1, t) = 0, & t > 0, \\ u(x, 0) = u_0(x), & t = 0, \quad 0 < x < 1, \end{cases} \quad (3.1)$$

where,  $\varepsilon$  is the coefficient that depends on density, thermal conductivity and capacity of material.  $u(0, t) = u(1, t) = 0$  is the boundary conditions, and  $u(x, 0) = u_0(x)$  is the initial conditions. As a potential case, the initial condition is as follow,

$$u_0(x) = \sin \pi x + m^2 A \sin m \pi x. \quad (3.2)$$

Thus, the analytical solution of Eq. (3.2) is written in an explicit form,

$$u(x, t) = e^{-\varepsilon \pi^2 t} \sin \pi x + m^2 A e^{-m^2 \varepsilon \pi^2 t} \sin 3 \pi x. \quad (3.3)$$

Here,  $m = 3$ ,  $A = 0.06$  is specified in all cases in this paper.

Decomposing the variable of  $u(x,t)$  is stated as follow,

$$\vec{u}(\vec{x},t) = \sum_{k=1}^{N_t} a_k(t) \vec{\zeta}_k(\vec{x}), \tag{3.4}$$

where,  $a_k$  is the coefficient that is subjected to the Galerkin projection,

$$G_l = \dot{a}_l + \varepsilon \sum_{k=1}^{N_t} a_k \int_0^1 \zeta_l' \zeta_k' dx, \tag{3.5}$$

and  $\zeta_l \in \mathfrak{R}$  is the unknown basis to be determined. By the initial condition,  $a_l(0)$  is satisfied as

$$a_l(0) = \int_0^1 u_0 \zeta_l dx. \tag{3.6}$$

The residue of the one-dimensional heat transfer equation is taken as,

$$R_k = \sum_{k=1}^{N_t} \dot{a}_k \zeta_k - \varepsilon \sum_{k=1}^{N_t} a_k \zeta_k''. \tag{3.7}$$

According to the methodology proposed in Section 2, the forth term at the right hand side of Eq. (2.5) is taken as optimal functional condition, and let  $\mu_4 = 1$ , such that,

$$J(\xi) = \int_0^T \sum_{l=1}^{N_t} |(\zeta_l, R_k)| dt = \int_0^T \sum_{l=1}^{N_t} \left| \dot{a}_l + \varepsilon \sum_{k=1}^{N_t} a_k \int_0^1 \zeta_l' \zeta_k' dx \right| dt. \tag{3.8}$$

Two solving strategies, A and B, are used, namely,

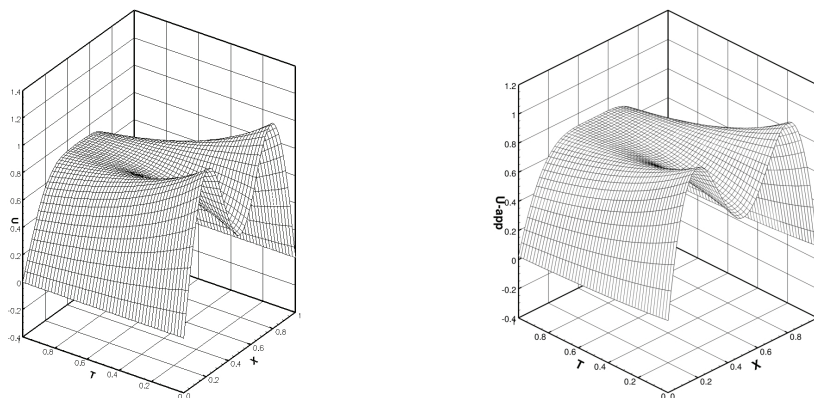
$$J^A(\xi) = \int_0^T \left( \sum_{l=1}^{N_t} \dot{a}_l + \varepsilon \sum_{k,l=1}^{N_t} a_k \int_0^1 \zeta_l' \zeta_k' dx \right) dt, \tag{3.9a}$$

$$J^B(\xi) = \int_0^T \left( - \sum_{l=1}^{N_t} \dot{a}_l - \varepsilon \sum_{k,l=1}^{N_t} a_k \int_0^1 \zeta_l' \zeta_k' dx \right) dt. \tag{3.9b}$$

The Lagrangian multiplier  $\lambda$  and the penalty function  $\mu$  are introduced to remove the constrains of the Galerkin projection equation and the orthogonal condition, respectively. The generalized optimal functional is obtained as follow,

$$J^{gA}(\xi) = J^A + \int_0^T \sum_{l=1}^{N_t} \lambda_l G_l dt + \sum_{k,l=1, k \leq l}^{N_t} \mu \left( \int_0^1 \zeta_k \zeta_l dx - \delta_{kl} \right)^2, \tag{3.10a}$$

$$J^{gB}(\xi) = J^B + \int_0^T \sum_{l=1}^{N_t} \lambda_l G_l dt + \sum_{k,l=1, k \leq l}^{N_t} \mu \left( \int_0^1 \zeta_k \zeta_l dx - \delta_{kl} \right)^2. \tag{3.10b}$$



(a) Exact solution for  $m = 3, A = 0.06$  corresponding to Eq. (3.3)      (b) POT-WR solution for Fourier polynomials

Figure 1: Exact solutions of Eq. (3.3) and POT-WR solutions of Eq. (3.1) for strategy A.

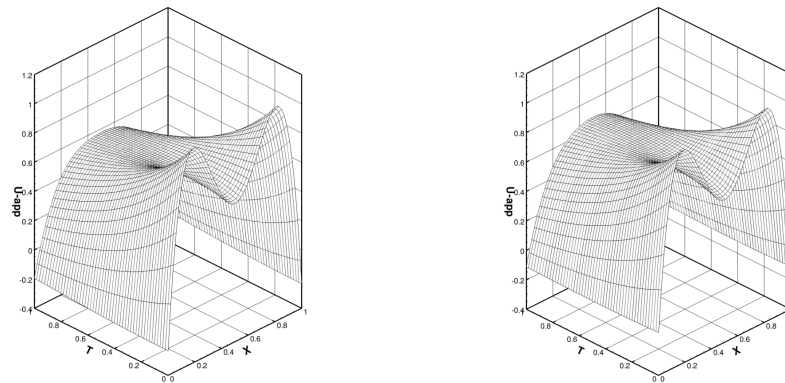
By using the extreme principle, taking variational operation of  $J^{g^A}(\xi), J^{g^B}(\xi)$ , and letting  $\delta J^{g^A}(\xi) = 0, \delta J^{g^B}(\xi) = 0$ , thus, the corresponding terms for the strategy A are obtained as

$$\left\{ \begin{array}{l} \dot{\lambda}_l = \sum_{k=1}^{N_t} (\varepsilon + \varepsilon \lambda_k) \int_0^1 \xi_k' \xi_l' dx, \\ 4\mu \xi_l \left( \int_0^1 \xi_l^2 dx - 1 \right) + \sum_{k=1, k \neq l}^{N_t} 2\mu \xi_k \left( \int_0^1 \xi_k \xi_l dx \right) - (\lambda_l(0) + 1) u_0 \\ - \sum_{k=1}^{N_t} \xi_k'' \int_0^T (\varepsilon a_l + \varepsilon a_k) dt - \sum_{k=1}^{N_t} \varepsilon \xi_k'' \int_0^T (\lambda_k a_l + \lambda_l a_k) dt = 0, \\ \dot{a}_l + \varepsilon \sum_{k=1}^{N_t} a_k \int_0^1 \xi_l' \xi_k' dx = 0. \end{array} \right. \quad (3.11)$$

For the strategy B as

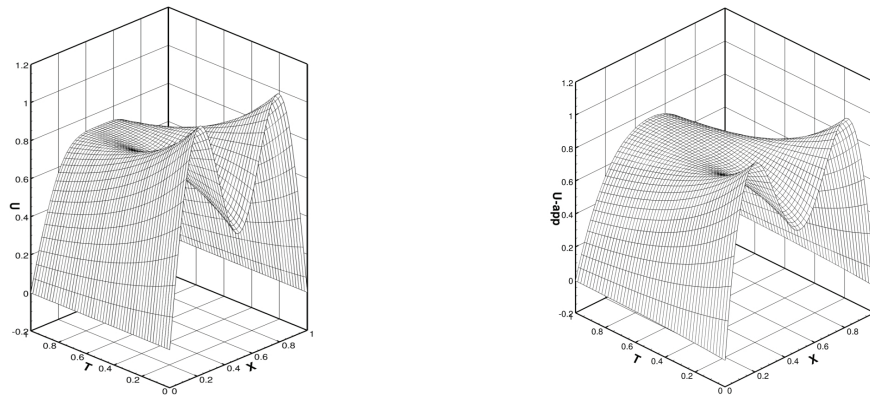
$$\left\{ \begin{array}{l} \dot{\lambda}_l = \sum_{k=1}^{N_t} (\varepsilon \lambda_k - \varepsilon) \int_0^1 \xi_k' \xi_l' dx, \\ 4\mu \xi_l \left( \int_0^1 \xi_l^2 dx - 1 \right) + \sum_{k=1, k \neq l}^{N_t} 2\mu \xi_k \left( \int_0^1 \xi_k \xi_l dx \right) + (1 - \lambda_l(0)) u_0 \\ + \sum_{k=1}^{N_t} \xi_k'' \int_0^T (\varepsilon a_l + \varepsilon a_k) dt - \sum_{k=1}^{N_t} \varepsilon \xi_k'' \int_0^T (\lambda_k a_l + \lambda_l a_k) dt = 0, \\ \dot{a}_l + \varepsilon \sum_{k=1}^{N_t} a_k \int_0^1 \xi_l' \xi_k' dx = 0. \end{array} \right. \quad (3.12)$$

For the sake of convenience to compare with the exact solution, the order number of the truncation is taken as two, namely,  $N_t = 2$ . The results of the local solutions for the



(a) POT-WR solution for Legendre polynomials (b) POT-WR solution for Chebyshev polynomials

Figure 2: Exact solutions of Eq. (3.3) and POT-WR solutions of Eq. (3.1) for strategy A.

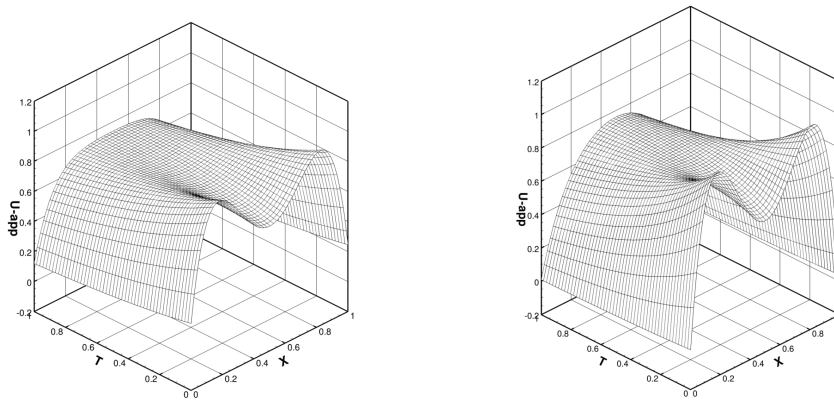


(a) Exact solution for  $m=3, A=0.06$  corresponding to Eq. (3.3) (b) POT-WR solution for Fourier polynomials

Figure 3: Exact solutions of Eq. (3.3) and POT-WR solutions of Eq. (3.1) for strategy B.

strategies A and B are shown in Figs. 1-4, respectively. Fig. 1(a) and Fig. 3(a) illustrate the exact solutions corresponding to Eq. (3.3). Figs. 1(b) to 2(b) illustrate the local optimal solutions of Eq. (3.1) for the strategy A. Figs. 3(b) to 4(b) are solutions for the strategy B. It is clear from Figs. 1-4 that the local optimal solutions based on the POT-WR method converge well into the exact solutions for two strategies. For the strategy A, the error on the Legendre polynomials is 3.0935%, which concentrates on the boundary as shown in Fig. 2(a). Fig. 1(b) denotes that the solution on the Fourier polynomials is more flat in curves. For the strategy B, the error on the Legendre polynomials is the same to the Fourier polynomials for the strategy A. The details of the comparisons are listed in Table 1.

From Figs. 5-7, it is seen that the relationships between the different initial bases and



(a) POT-WR solution for Legendre polynomials (b) POT-WR solution for Chebyshev polynomials

Figure 4: Exact solutions of Eq. (3.3) and POT-WR solutions of Eq. (3.1) for strategy B.

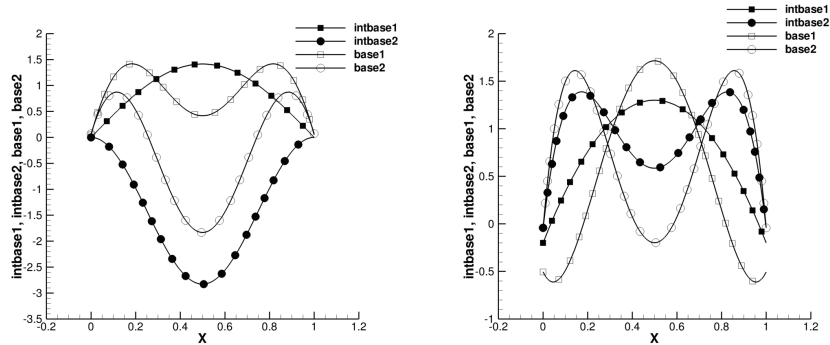
their local optimal bases are in contrast. The curves with solid symbol represent the initial basis, and others are the local optimal basis. The local optimal basis is totally different from the initial one. Especially, the first and second order optimal bases are almost symmetry in Figs. 5(b), 6(a), 7(a), and 7(b) for the Legendre and Chebyshev polynomials for two strategies. For the local optimal search, the different initial basis results in the different shape of the local optimal basis. It demonstrates that the local optimal basis is very sensitive to the initial basis.

It is necessary to obtain the global optimal basis for constructing a model of the optimal low-dimensional dynamical system, and eliminating the sensitivity to the initial basis. Figs. 8-14 show the investigations of the global optimal search. Figs. 8-10 shows that a tendency of the error and residue of Eq. (3.1) with the number of search. The red lines represent the residue of Eq. (3.1) in meaning of time averaging, and converge to zero when the error of the solution of Eq. (3.1) tends to be stable for two strategies. The tendency is the same to other cases.

The global optimal basis in different cases is shown in Figs. 11-14. The curve with solid square symbol is the first order basis, and the other is the second order one. The optimal bases in the Fourier polynomials are shown in Figs. 11(a) and 12(b), and they

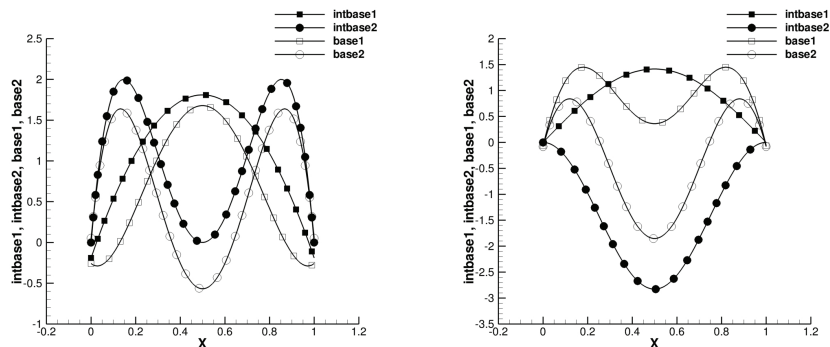
Table 1: Local and global errors of heat transfer equation for different initial bases (%).

Case	$N$	Initial Basis	Local Error (%)	Global Error (%)
A	2	Fourier	0.4950	0.3196
	2	Legendre	3.0935	0.6532
	2	Chebyshev	1.0100	0.5328
B	2	Fourier	0.2592	0.1890
	2	Legendre	2.5522	0.5278
	2	Chebyshev	0.6514	0.5542



(a) Fourier polynomials versus corresponding local optimal bases for strategy A  
 (b) Legendre polynomials versus corresponding local optimal bases for strategy A

Figure 5: Initial bases versus corresponding local optimal bases of Eq. (3.1) for two strategies.



(a) Chebyshev polynomials versus corresponding local optimal bases for strategy A  
 (b) Fourier polynomials versus corresponding local optimal bases for strategy B

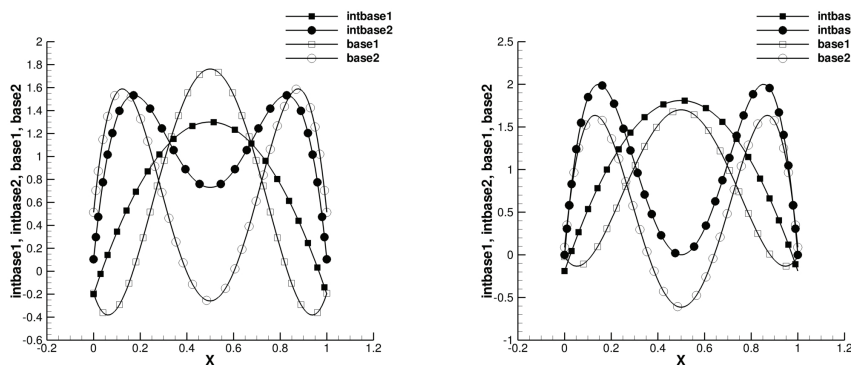
Figure 6: Initial bases versus corresponding local optimal bases of Eq. (3.1) for two strategies.

converge exactly on the boundary, comparing with the Legendre and Chebyshev polynomials. So, it is concluded that the error on the Fourier polynomials is smallest, and the global optimal basis is insensitive to the iterative initial basis.

### 3.3 Burgers' equation

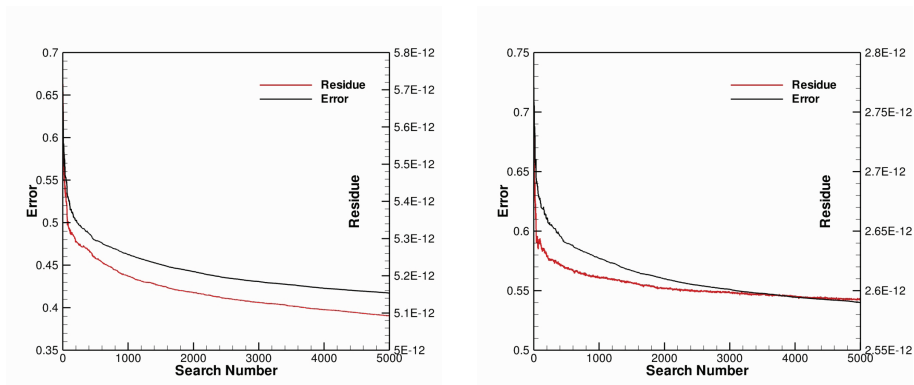
The Burgers' equation with nonlinear term is taken as the second example, and it is stated as

$$\begin{cases} \frac{\partial u}{\partial t} + u \frac{\partial u}{\partial x} = \nu \frac{\partial^2 u}{\partial x^2}, & t > 0, \quad 0 < x < 1, \\ u(0, t) = u(1, t) = 0, & 0 < t \leq 1, \\ u(x, 0) = u_0(x), & 0 < x < 1, \end{cases} \quad (3.13)$$



(a) Legendre polynomials versus corresponding local optimal bases for strategy B (b) Chebyshev polynomials versus corresponding local optimal bases for strategy B

Figure 7: Initial bases versus corresponding local optimal bases of Eq. (3.1) for two strategies.



(a) Fourier error and weighted residue of Eq. (3.1) for strategy A (b) Legendre error and weighted residue of Eq. (3.1) for strategy A

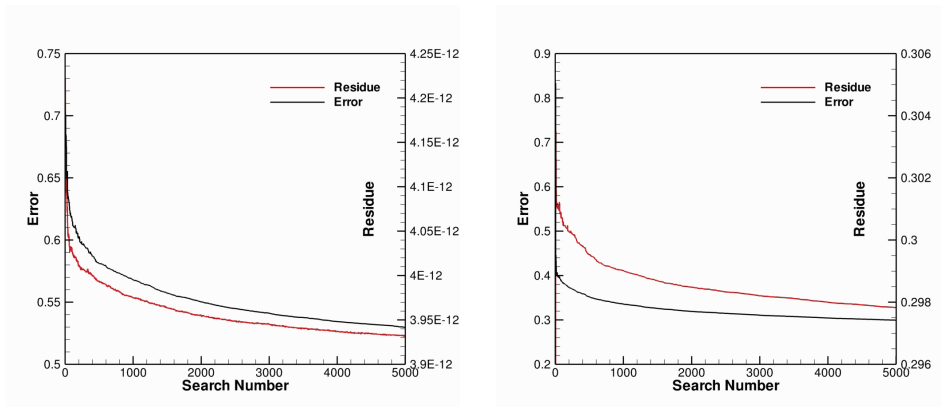
Figure 8: Error and weighted residue of Eq. (3.1) for different convergent criterions.

where,  $\nu$  is the viscosity coefficient.  $u(0,t) = u(1,t) = 0$  is the boundary conditions, and  $u(x,0) = u_0(x)$  is the initial conditions. As a potential case under consideration, an initial condition is applied as follow,

$$u_0(x) = 0.5\sin \pi x + \sin 2\pi x + 1.5\sin 3\pi x. \tag{3.14}$$

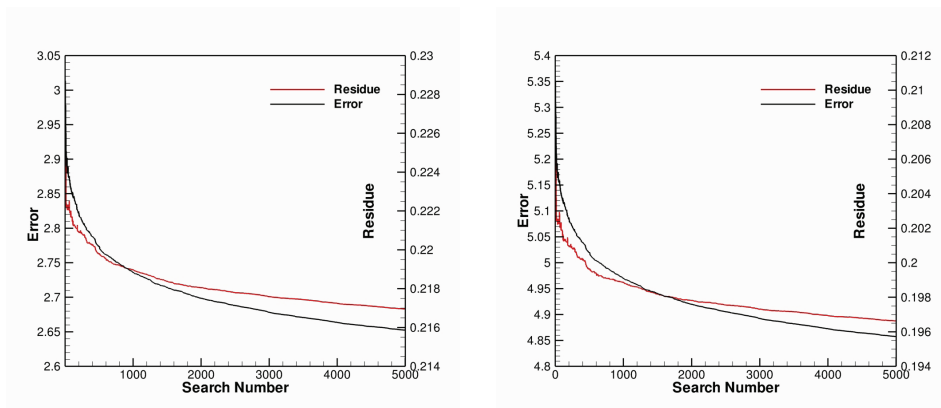
According to the Cole-Hopf transformation, the analytical solution of Eq. (3.13) with the initial condition of Eq. (3.14) is yielded in form,

$$u(x,t) = 2\nu\pi \frac{\sum_{n=1}^{+\infty} nA_n e^{-n^2\pi^2\nu t} \sin n\pi x}{A_0 + \sum_{n=1}^{+\infty} A_n e^{-n^2\pi^2\nu t} \cos n\pi x}, \tag{3.15}$$



(a) Chebyshev error and weighted residue of Eq. (3.1) for strategy A (b) Fourier error and weighted residue of Eq. (3.1) for strategy B

Figure 9: Error and weighted residue of Eq. (3.1) for different convergent criterions.



(a) Legendre error and weighted residue of Eq. (3.1) for strategy B (b) Chebyshev error and weighted residue of Eq. (3.1) for strategy B

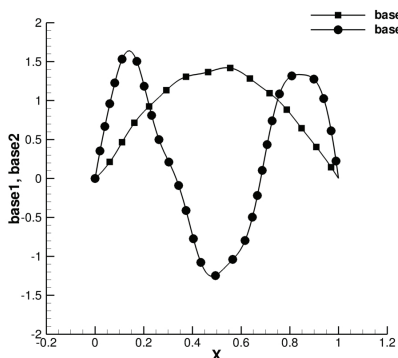
Figure 10: Error and weighted residue of Eq. (3.1) for different convergent criterions.

in which,

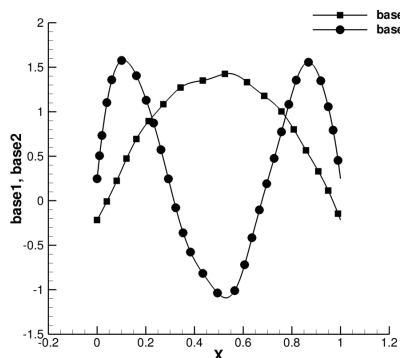
$$\begin{cases} A_0 = C \int_0^1 \exp \left[ -\frac{1}{2\nu} \int_0^x u_0(\xi) d\xi \right] dx, \\ A_n = 2C \int_0^1 \exp \left[ -\frac{1}{2\nu} \int_0^x u_0(\xi) d\xi \right] \cos n\pi x dx, \quad n = 1, 2, \dots \end{cases} \quad (3.16)$$

As an approximation of the solution, the variable of  $u(x,t)$  is expanded as,

$$u \approx \sum_{k=1}^{N_t} a_k(t) \xi_k(x), \quad (3.17)$$

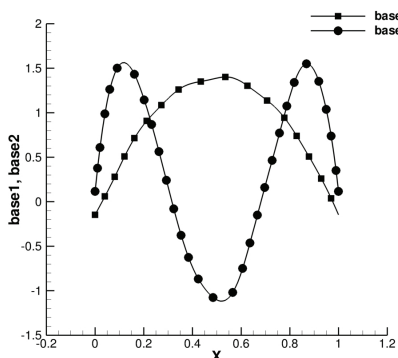


(a) Global optimal basis of Fourier polynomials for strategy A

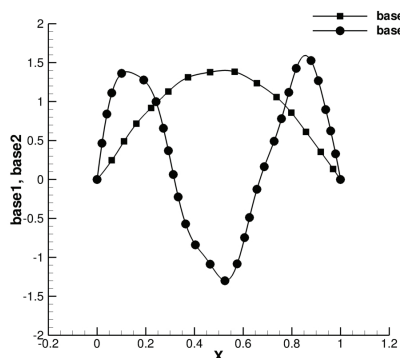


(b) Global optimal basis of Legendre polynomials for strategy A

Figure 11: Error and weighted residue of Eq. (3.1) for different convergent criterions.



(a) Global optimal basis of Chebyshev polynomials for strategy A



(b) Global optimal basis of Fourier polynomials for strategy B

Figure 12: Error and weighted residue of Eq. (3.1) for different convergent criterions.

where,  $a_k$  is the coefficient. By using the Galerkin projection, a formulation is obtained as

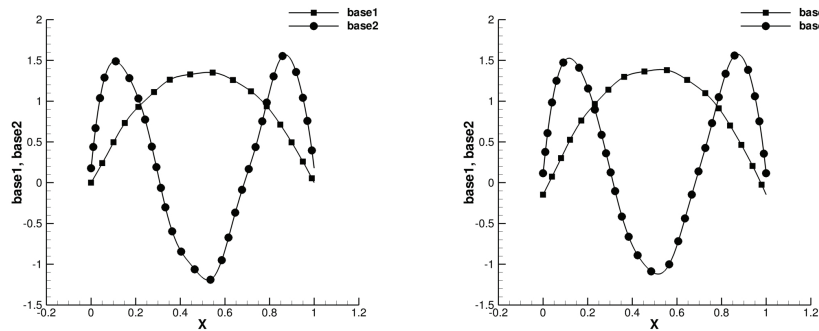
$$G_l = \dot{a}_l + \sum_{k,m=1}^{N_l} a_k a_m \int_0^1 \zeta_k \zeta_l \zeta_m' dx + \nu \sum_{k=1}^{N_l} a_k \int_0^1 \zeta_k' \zeta_l' dx, \tag{3.18}$$

and  $\zeta_l \in \mathfrak{R}$  is the unknown basis to be determined. By the initial condition,  $a_l(0)$  is satisfied as,

$$a_l(0) = \int_0^1 u_0 \zeta_l dx. \tag{3.19}$$

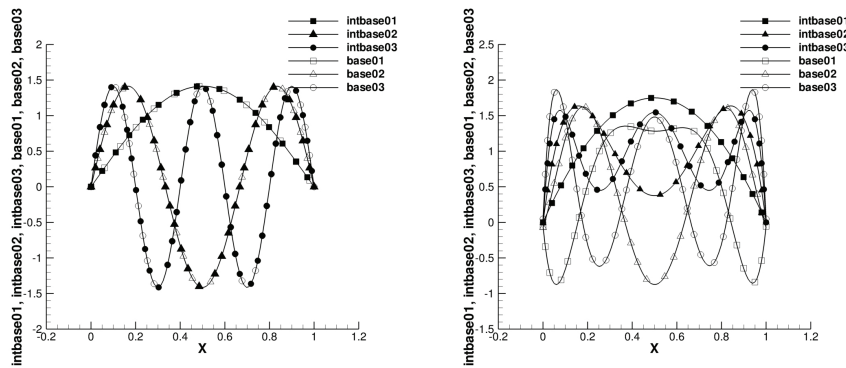
Moreover, the residue of the Burgers' equation is taken as,

$$R_k = \sum_{k=1}^{N_l} \dot{a}_k \zeta_k + \sum_{k,m=1}^{N_l} a_k a_m \zeta_k \zeta_m' - \nu \sum_{k=1}^{N_l} a_k \zeta_k''. \tag{3.20}$$



(a) Global optimal basis of Legendre polynomials for strategy B (b) Global optimal basis of Chebyshev polynomials for strategy B

Figure 13: Global optimal bases of Eq. (3.1) for different convergent criteria.



(a) Fourier polynomials versus corresponding local optimal bases for strategy A (b) Legendre polynomials versus corresponding local optimal bases for strategy A

Figure 14: Initial bases versus corresponding local optimal bases of Eq. (3.13)  $\nu=0.02$  for two strategies.

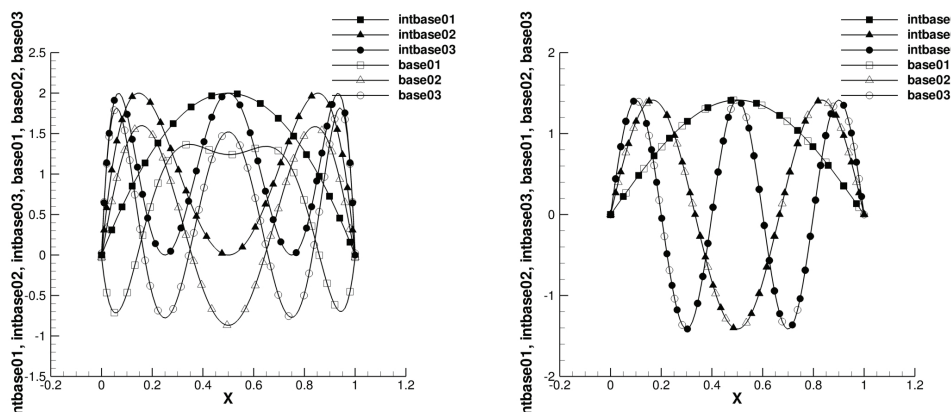
According to the method proposed in Section 2, the fourth term of the right hand side of Eq. (2.5) is taken as the optimal functional condition, and set  $\mu_4 = 1$ , such that,

$$J(\xi) = \int_0^T \sum_{l=1}^{N_t} |(\xi_l, R_k)| dt = \int_0^T \sum_{l=1}^{N_t} \left| \dot{a}_l + \sum_{k,l=1}^{N_t} a_k a_m \int_0^1 \xi_k \xi_l \xi'_m dx + \nu \sum_{k=1}^{N_t} a_k \int_0^1 \xi'_l \xi'_k dx \right| dt. \quad (3.21)$$

By the same way, two solving strategies, A and B, are used, respectively,

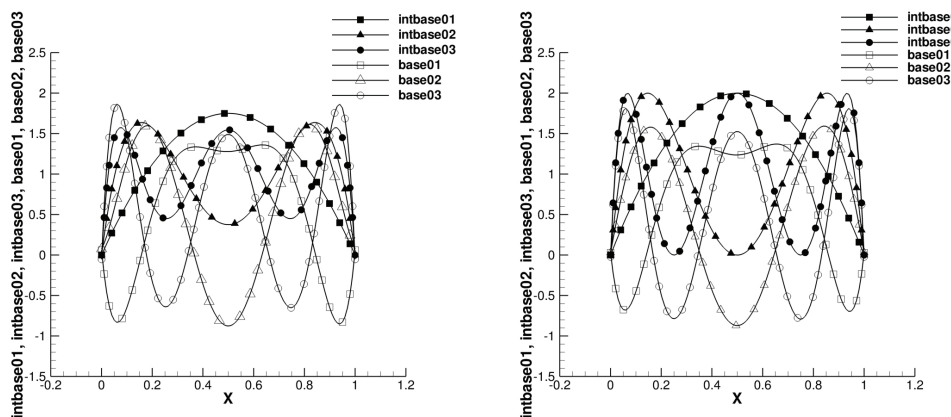
$$J^A(\xi) = \int_0^T \left( \sum_{l=1}^{N_t} \dot{a}_l + \sum_{k,l=1}^{N_t} a_k a_l \int_0^1 \xi_k \xi_l \xi'_m dx + \nu \sum_{l,k=1}^{N_t} a_k \int_0^1 \xi'_l \xi'_k dx \right) dt, \quad (3.22a)$$

$$J^B(\xi) = \int_0^T \left( - \sum_{l=1}^{N_t} \dot{a}_l - \sum_{k,l=1}^{N_t} a_k a_l \int_0^1 \xi_k \xi_l \xi'_m dx - \nu \sum_{l,k=1}^{N_t} a_k \int_0^1 \xi'_l \xi'_k dx \right) dt. \quad (3.22b)$$



(a) Chebyshev polynomials versus corresponding local optimal bases for strategy A (b) Fourier polynomials versus corresponding local optimal bases for strategy B

Figure 15: Initial bases versus corresponding local optimal bases of Eq. (3.13)  $\nu=0.02$  for two strategies.



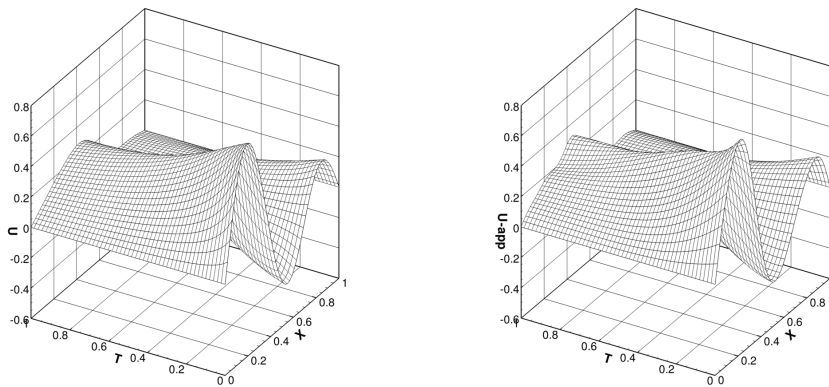
(a) Legendre polynomials versus corresponding local optimal bases for strategy B (b) Chebyshev polynomials versus corresponding local optimal bases for strategy B

Figure 16: Initial bases versus corresponding local optimal bases of Eq. (3.13)  $\nu=0.02$  for two strategies.

The Lagrangian multiplier  $\lambda$  and the penalty function  $\mu$  are used to remove the constraints of the Galerkin projection equation and the orthogonal condition, respectively. The generalized optimal functions are obtained as follow,

$$J^{g^A}(\xi) = J^A + \int_0^T \sum_{l=1}^{N_t} \lambda_l G_l dt + \sum_{k,l=1, k \leq l}^{N_t} \mu \left( \int_0^1 \xi_k \xi_l dx - \delta_{kl} \right)^2, \quad (3.23a)$$

$$J^{g^B}(\xi) = J^B + \int_0^T \sum_{l=1}^{N_t} \lambda_l G_l dt + \sum_{k,l=1, k \leq l}^{N_t} \mu \left( \int_0^1 \xi_k \xi_l dx - \delta_{kl} \right)^2. \quad (3.23b)$$



(a) Exact solution for  $\nu=0.02$  corresponding to Eq. (3.15)      (b) POT-WR solution for Fourier polynomials

Figure 17: Exact solution of Eq. (3.15) and global POT-WR solution of Eq. (3.13) for strategy A  $\nu=0.02$ .

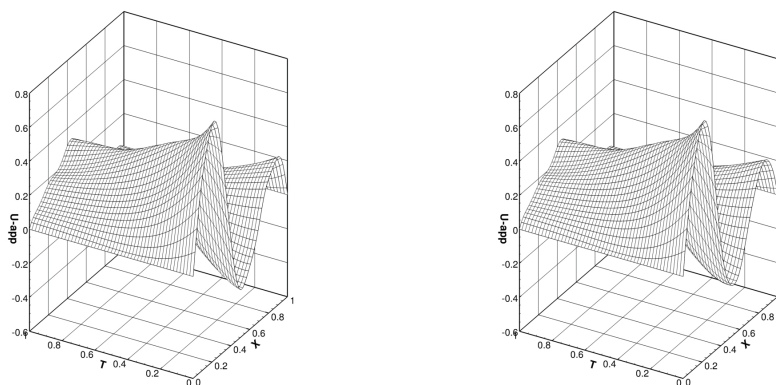
Taking variational operation of  $J^{g^A}(\xi)$ ,  $J^{g^B}(\xi)$ , and letting  $\delta J^{g^A}(\xi) = 0$ ,  $\delta J^{g^B}(\xi) = 0$ , thus, for the strategy A, it is obtained as

$$\left\{ \begin{aligned} \dot{\lambda}_l &= \sum_{k,m=1}^{N_t} (1 + \lambda_k) a_m \left( \int_0^1 \xi_l \xi_k \xi'_m dx + \int_0^1 \xi_k \xi_m \xi'_l dx \right) + \nu \sum_{k=1}^{N_t} (1 + \lambda_k) \int_0^1 \xi'_k \xi'_l dx, \\ 0 &= 4\mu \xi_l \left( \int_0^1 \xi_l^2 dx - 1 \right) - (1 + \lambda_l(0)) u_0 - \sum_{k=1}^{N_t} \nu \xi''_k \int_0^T ((1 + \lambda_k) a_l + (1 + \lambda_l) a_k) dt \\ &\quad + \sum_{k,l=1, k \leq l}^{N_t} 2\mu \xi_k \left( \int_0^1 \xi_k \xi_l dx \right) + \sum_{k,m=1}^{N_t} \xi_k \xi'_m \int_0^T ((1 + \lambda_l) a_k a_m - (1 + \lambda_m) a_k a_l) dt, \\ 0 &= \dot{a}_l + \sum_{k,m=1}^{N_t} a_k a_m \int_0^1 \xi_k \xi_l \xi'_m dx + \nu \sum_{k=1}^{N_t} a_k \int_0^1 \xi'_k \xi'_l dx, \end{aligned} \right. \quad (3.24)$$

and for the strategy B,

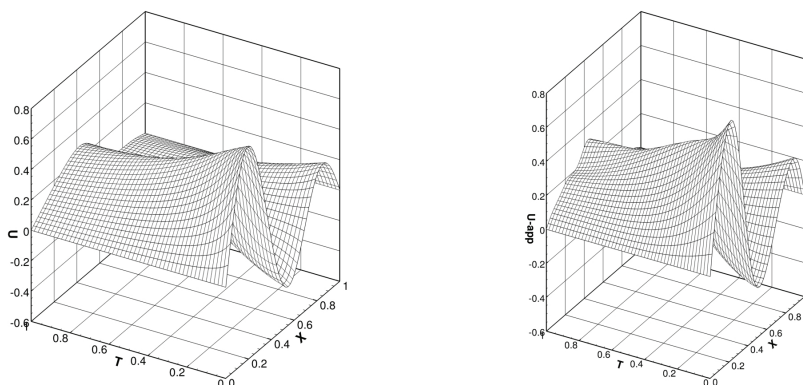
$$\left\{ \begin{aligned} \dot{\lambda}_l &= \sum_{k,m=1}^{N_t} (\lambda_k - 1) a_m \left( \int_0^1 \xi_l \xi_k \xi'_m dx - \int_0^1 \xi_k \xi_m \xi'_l dx \right) + \nu \sum_{k=1}^{N_t} (\lambda_k - 1) \int_0^1 \xi'_k \xi'_l dx, \\ 0 &= 4\mu \xi_l \left( \int_0^1 \xi_l^2 dx - 1 \right) + (1 - \lambda_l(0)) u_0 + \sum_{k=1}^{N_t} \nu \xi''_k \int_0^T ((1 - \lambda_k) a_l + (1 - \lambda_l) a_k) dt \\ &\quad + \sum_{k,l=1, k \leq l}^{N_t} 2\mu \xi_k \left( \int_0^1 \xi_k \xi_l dx \right) + \sum_{k,m=1}^{N_t} \xi_k \xi'_m \int_0^T ((1 - \lambda_m) a_k a_l - (1 - \lambda_l) a_k a_m) dt, \\ 0 &= \dot{a}_l + \sum_{k,m=1}^{N_t} a_k a_m \int_0^1 \xi_k \xi_l \xi'_m dx + \nu \sum_{k=1}^{N_t} a_k \int_0^1 \xi'_k \xi'_l dx. \end{aligned} \right. \quad (3.25)$$

In order to catch a  $N$ -wave shock of the Burgers' equation when  $\nu$  is small, the order number of the truncation is taken as three, namely,  $N_t = 3$ . Figs. 14-16 illustrates the contrast



(a) POT-WR solution for Legendre polynomials

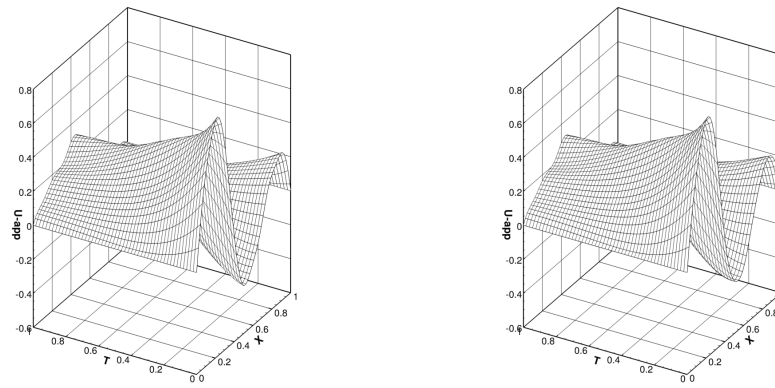
(b) POT-WR solution for Chebyshev polynomials

Figure 18: Exact solution of Eq. (3.15) and global POT-WR solution of Eq. (3.13) for strategy A  $\nu=0.02$ .(a) Exact solution for  $\nu=0.02$  corresponding to Eq. (3.15)

(b) POT-WR solution for Fourier polynomials

Figure 19: Exact solution of Eq. (3.15) and global POT-WR solution of Eq. (3.13) for strategy B  $\nu=0.02$ .

between the initial bases and local optimal bases of Eq. (3.13) for the different strategies under  $\nu=0.02$ . The curves with solid symbol are the initial basis, and others are the local optimal basis. The solutions of the local optimal bases based on the different initial bases for the Legendre and Chebyshev polynomials are basically same for two strategies. But, for the Fourier polynomials, it is seen from Fig. 14(a) and Fig. 15(b) that the local optimal basis have the exactly same shape to the initial basis. The reason is that the Fourier initial basis belongs to a part of the exact solution of the Burgers' equation, which is optimal one. However, it is noted that the local optimal bases are not able to catch the  $N$ -wave shock of the Burgers' equation, even neither for the Fourier polynomials. Thus, it is necessary to find out the global optimal basis that can catch the main dynamical characteristics of the Burgers' equation.



(a) POT-WR solution for Legendre polynomials (b) POT-WR solution for Chebyshev polynomials

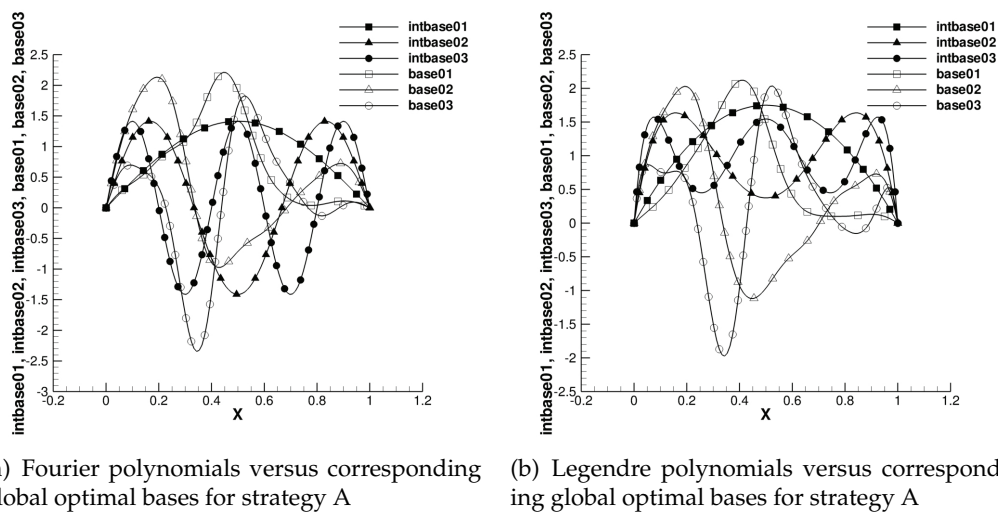
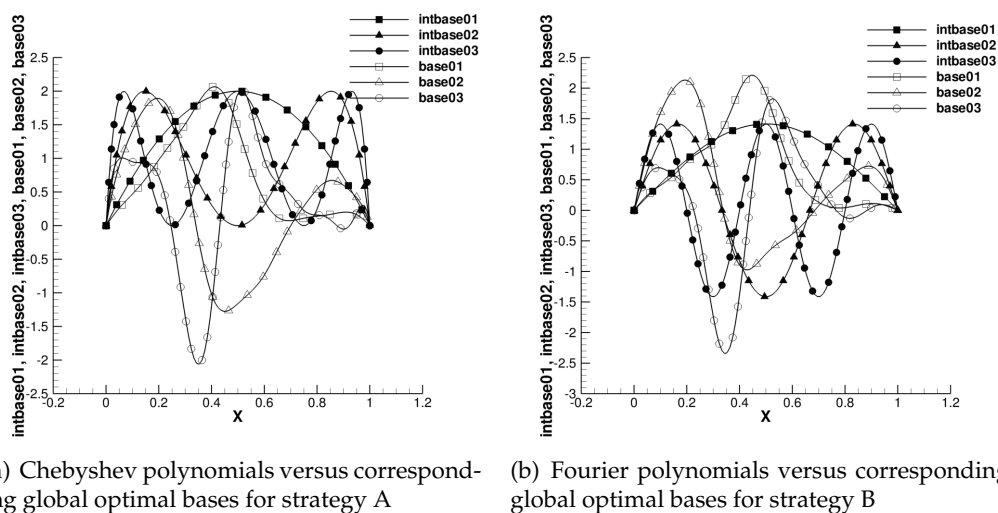
Figure 20: Exact solution of Eq. (3.15) and global POT-WR solution of Eq. (3.13) for strategy B  $\nu = 0.02$ .

The errors between exact and approximate solutions on POD, the Fourier polynomials, DOT, and POT-WR are listed in Table 2. It is seen that the results obtained by the POT-WR method have much better accuracy than the other methods. From Figs. 17-20, the global optimal solutions converge well into exact solutions at  $\nu = 0.02$ . Not only the  $N$  shape shock but also the distortion along the evolution of time is well caught for two strategies. Furthermore, it is clear in Figs. 21-23 that the third order basis represented by a curve with circle shows the characters of the  $N$  shape shock. Comparing the results of the local optimal bases shown in Figs. 14-16, the global optimal bases are independent of the initial basis.

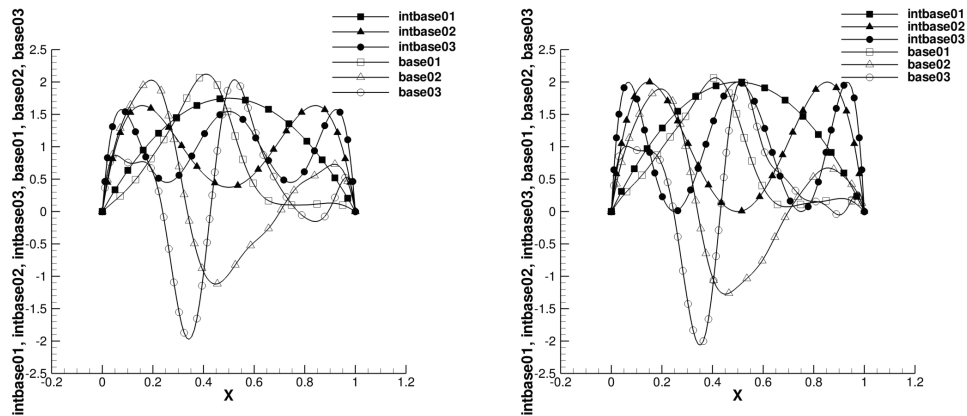
Convergent criterion is a critical condition for the global optimal search. From Figs. 24-26, the difference between the exact and approximate solutions is taken as the convergent criterion. The residue of Eq. (3.13) tends to stabilization as the error of Eq. (3.13) converges to zero for two strategies. From Figs. 27-28, in order to investigate the margin of the error when the smallest weighted residue is found out after 5000 times searches,

Table 2: Errors for Fourier polynomials, POD, DOT, and POT-WR (%).

Base No.	Method	$\nu = 0.1$	$\nu = 0.05$	$\nu = 0.02$
3	Fourier [19]	3.730	13.084	40.306
	POD [19]	1.214	3.788	16.241
	DOT [19]	1.061	3.418	8.799
	POT-WR-A	0.105	0.172	0.343
	POT-WR-B	0.105	0.172	0.343
4	Fourier [19]	0.897	2.955	17.650
	POD [19]	0.333	1.359	7.339
	DOT [19]	0.312	1.276	5.640
	POT-WR-A	0.056	0.121	0.300
	POT-WR-B	0.056	0.121	0.300

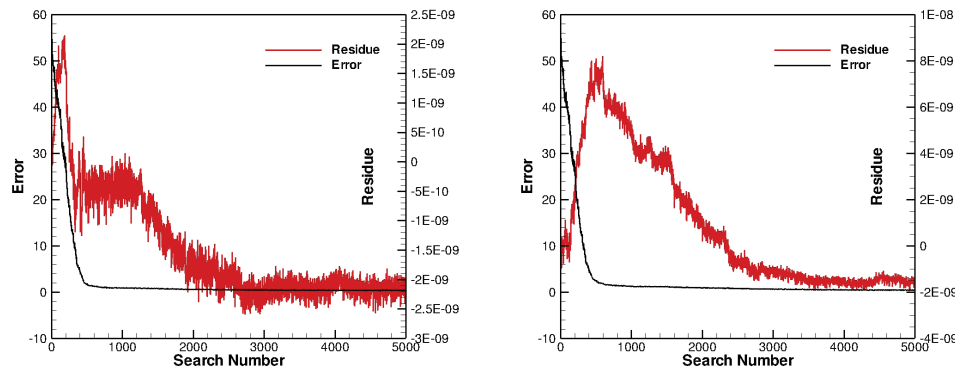
Figure 21: Initial bases versus corresponding local optimal bases of Eq. (3.13)  $\nu=0.02$  for two strategies.Figure 22: Initial bases versus corresponding local optimal bases of Eq. (3.13)  $\nu=0.02$  for two strategies.

the weighted residue based on time averaging is taken as the convergent criterion. The margin of the error is limited when the residue is convergent for two strategies. The errors indicated in Figs. 27-28 tend to be stable for both strategy A and B after about 2000 times search. Even though the error is still large, the method on the weighted residue bounds the error effectively. However, as mentioned in Section 1, the error is divergent when the residue is taken as the convergent criterion of the POT method. Thus, from the view of computational mechanics, the weighted residue method seems to be better than a method of directly making residue zero.



(a) Legendre polynomials versus corresponding global optimal bases for strategy B (b) Chebyshev polynomials versus corresponding global optimal bases for strategy B

Figure 23: Initial bases versus global optimal bases of Eq. (3.13)  $\nu=0.02$  for two strategies.

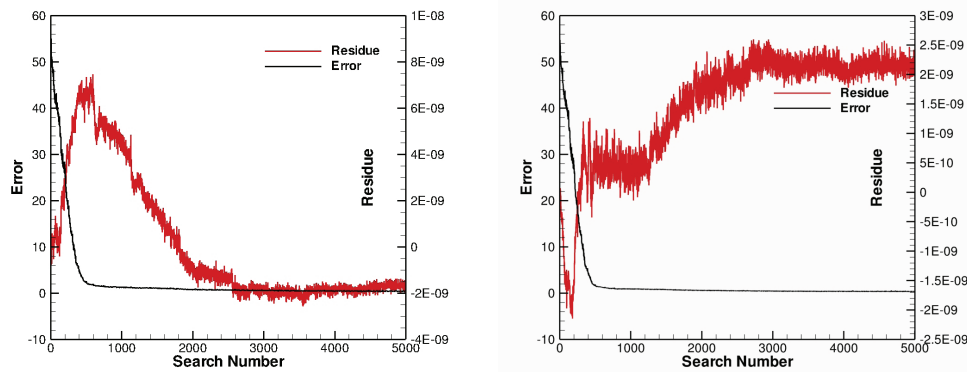


(a) Fourier error and weighted residue of Eq. (3.13) for strategy A (b) Legendre error and weighted residue of Eq. (3.13) for strategy A

Figure 24: Initial bases versus corresponding local optimal bases of Eq. (3.13)  $\nu=0.02$  for two strategies.

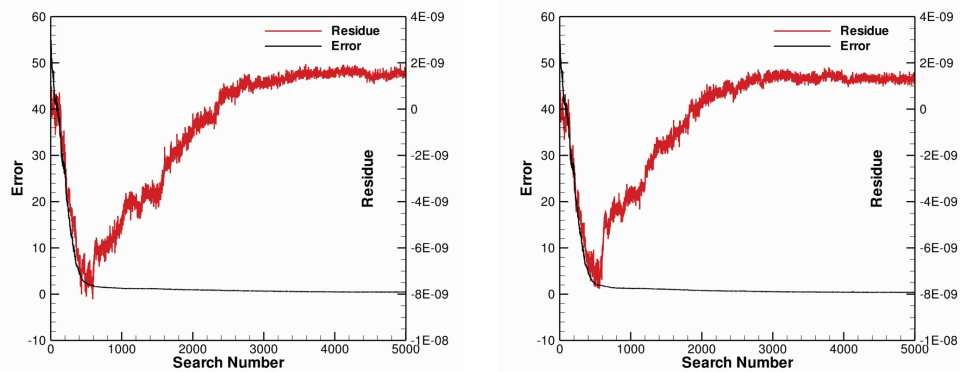
## 4 Conclusions

The weighted residue of the system under consideration is taken as a changing optimal control condition of POT to solve the system by low dimensional models, which allows to construct a optimal basis for the solution without a given database. The conjugate gradient algorithm is used to solve the equation. One-dimensional heat transfer equation and Burgers' equation are taken as examples of solving the linear and nonlinear PDEs, respectively. The results show that the novel method (POT-WR) proposed in this paper is quit efficiency of approximating the exact solutions with a few truncations. The global optimal searches make a great improvement of the local optimal solutions. The investigation



(a) Chebyshev error and weighted residue of Eq. (3.13) for strategy A

(b) Fourier error and weighted residue of Eq. (3.13) for strategy B

Figure 25: Initial bases versus corresponding local optimal bases of Eq. (3.13)  $\nu = 0.02$  for two strategies.

(a) Legendre error and weighted residue of Eq. (3.13) for strategy B

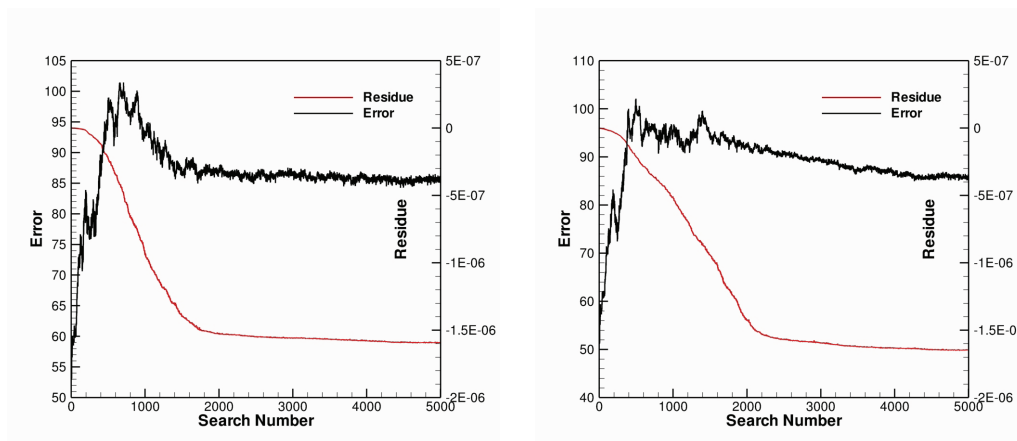
(b) Chebyshev error and weighted residue of Eq. (3.13) for strategy B

Figure 26: Error and the weighted residue of Eq. (3.13) for different convergent criteria.

of the convergent criterion of the global optimal searches illustrates that the application of the weighted residue of the equation under consideration as the convergent criterion is an effective way to bound the error of the solution. The method proposed in this paper can be used for solving high dimensional problems for turbulence flow.

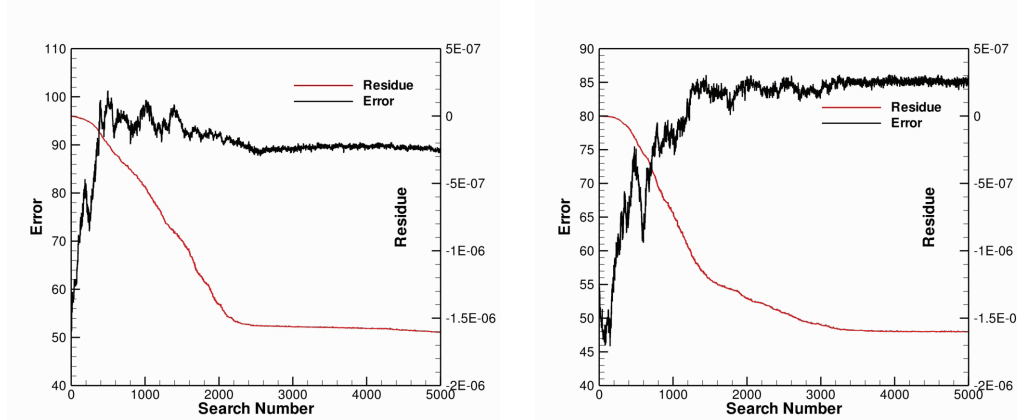
## Acknowledgments

The work described in this paper was supported by Natural Science Foundation of China under Great Nos. 11072053 and 11372068, and the National Basic Research Program of China under Grant No. 2014CB74410.



(a) Fourier error and weighted residue of E-q. (3.13) for strategy A      (b) Legendre error and weighted residue of E-q. (3.13) for strategy A

Figure 27: Initial bases versus corresponding local optimal bases of Eq. (3.13)  $\nu=0.02$  for two strategies.

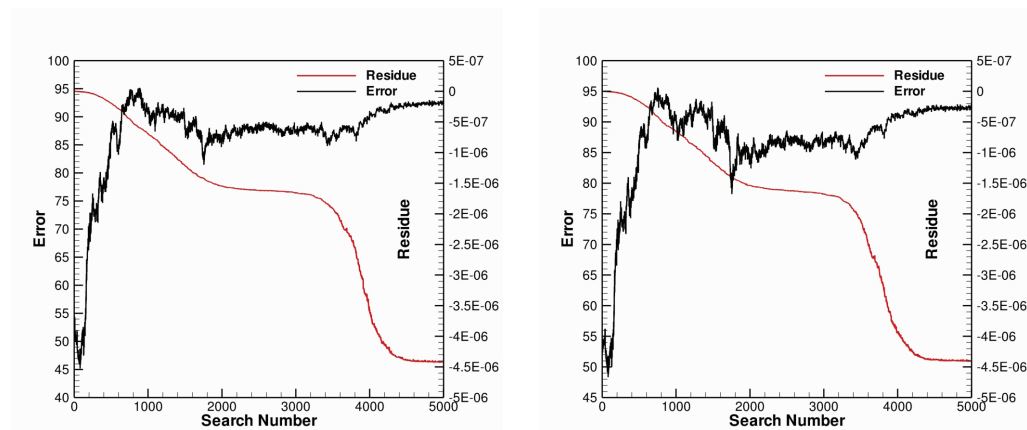


(a) Chebyshev error and weighted residue of E-q. (3.13) for strategy A      (b) Fourier error and weighted residue of E-q. (3.13) for strategy B

Figure 28: Initial bases versus corresponding local optimal bases of Eq. (3.13)  $\nu=0.02$  for two strategies.

## References

- [1] SAM T. ROWEIS AND LAWRENCE K. SAUL, *Nonlinear dimensionality reduction by locally linear embedding*, Science, 209 (2000), pp. 2323.
- [2] JOSHUA B. TENENBAUM, VIN DE SILVA AND JOHN C. LANGFORD, *A global geometric framework for nonlinear dimensionality reduction*, Science, 290 (2000), pp. 2319.
- [3] GABRIEL WĘCEL, ZIEMOWIT OSTROWSKI AND RYSZARD A. BIAŁECKI, *A novel approach of evaluating absorption line black body distribution function employing proper orthogonal decomposition*, J. Quantitative Spectroscopy Radiative Transfer, 111 (2010), pp. 309–317.
- [4] E. LIBERGE AND A. HAMDOUNI, *Reduced order modelling method via proper orthogonal decomposition (POD) for flow around an oscillating cylinder*, J. Fluids Structures, 26 (2010), pp.



(a) Legendre error and weighted residue of Eq. (3.13) for strategy B

(b) Chebyshev error and weighted residue of Eq. (3.13) for strategy B

Figure 29: Error and the weighted residue of Eq. (3.13) for different convergent criterions.

292–311.

- [5] MOHAMMADD KHALIL, SONDIPON ADHIKARI AND ABHIJIT SARKAR, *Linear system identification using proper orthogonal decomposition*, Mechanical Systems and Signal Processing, 21 (2007), pp. 3123–3145.
- [6] J. A. ATWELL AND B. B. KING, *Proper orthogonal decomposition for reduced basis feedback controllers for parabolic equations*, Math. Comput. Model., 33 (2001), pp. 1–19.
- [7] RÉMI BOURGUET, MARIANNA BRAZA AND ALAIN DERVIEUX, *Reduced-order modeling of transonic flows around an airfoil submitted to small deformations*, J. Comput. Phys., 230 (2011), pp. 159–184.
- [8] MARÍA-LUISA RAPÚN AND JOSÉ M. VEGA, *Reduced order models based on local POD plus Galerkin projection*, J. Comput. Phys., 229 (2010), pp. 3046–3063.
- [9] J. YVONNET, H. ZAHROUNI AND M. POTIER-FERRY, *A model reduction method for the post-buckling analysis of cellular microstructures*, Comput. Methods Appl. Mech. Eng., 197 (2007), pp. 265–280.
- [10] A. HAY, J. BORGGAARD, I. AKHTAR AND D. PELLETIER, *Reduced-order models for parameter dependent geometries based on shape sensitivity analysis*, J. Comput. Phys., 229 (2010), pp. 1327–1352.
- [11] MYKHAYLO KRASNYYK, MICHAEL MANGOLD AND ACHIM KIENLE, *Reduction procedure for parametrized fluid dynamics problems based on proper orthogonal decomposition and calibration*, Chemical Eng. Sci., 65 (2010), pp. 6238–6246.
- [12] IRINA KALASHNIKOVA, BART VAN BLOEMEN WAANDERS, SRINIVASAN ARUNAJATESAN AND MATTHEW BARONE, *Stabilization of projection-based reduced order models for linear time-invariant systems via optimization-based eigenvalue reassignment*, Comput. Methods Appl. Mech. Eng., 272 (2014), pp. 251–270.
- [13] ZHENDONG LUO, XIAOZHONG YANG AND YANJIE ZHOU, *A reduced finite difference scheme based on singular value decomposition and proper orthogonal decomposition for Burgers equation*, J. Comput. Appl. Math., 229 (2009), pp. 97–107.
- [14] D. ALONSO, A. VELAZQUEZ AND J. M. VEGA, *A method to generate computationally efficient reduced order models*, Comput. Methods Appl. Mech. Eng., 198 (2009), pp. 2683–2691.

- [15] XIAO-LONG WANG AND YAO-LIN JIANG, *Model order reduction methods for coupled systems in the time domain using Laguerre polynomials*, *Comput. Math. Appl.*, 62 (2011), pp. 3241–3250.
- [16] A. AMMAR, B. MOKDAD, F. CHINESTA AND R. KEUNINGS, *A new family of solvers for some classes of multidimensional partial differential equations encountered in kinetic theory modeling of complex fluids*, *J. Non-Newtonian Fluid Mech.*, 139 (2006), pp. 153–176.
- [17] A. AMMAR, B. MOKDAD, F. CHINESTA AND R. KEUNINGS, *A new family of solvers for some classes of multidimensional partial differential equations encountered in kinetic theory modelling of complex fluids Part II: Transient simulation using space-time separated representations*, *J. Non-Newtonian Fluid Mech.*, 144 (2007), pp. 98–121.
- [18] DAVID GONZÁLEZ, AMINE AMMAR, FRANCISCO CHINESTA AND ELÍAS CUETO, *Recent advances on the use of separated representations*, *Int. J. Numer. Methods Eng.*, 81 (2010), pp. 637–659.
- [19] CHUI JIE WU, *Large optimal truncated low-dimensional dynamical systems*, *Discrete and Continuous Dynamical Systems*, 2 (1996), pp. 559–583.
- [20] CH. HEYBERGER, P.-A. BOUCARD AND D. NÉRON, *A rational strategy for the resolution of parametrized problems in the PGD framework*, *Comput. Methods Appl. Mech. Eng.*, 259 (2013), pp. 40–49.
- [21] D. GONZÁLEZ, F. MASSON, F. POULHAON, A. LEYGUE, E. CUETO AND F. CHINESTA, *Proper generalized decomposition based dynamic data driven inverse identification*, *Math. Comput. Simulation*, 82 (2012), pp. 1677–1695.
- [22] A. DUMON, C. ALLERY AND A. AMMAR, *Proper general decomposition (PGD) for the resolution of Navier-Stokes equations*, *J. Comput. Phys.*, 230 (2011), pp. 1387–1407.
- [23] F. CHINESTA, A. AMMAR, A. LEYGUE AND R. KEUNINGS, *An overview of the proper generalized decomposition with applications in computational rheology*, *J. Non-Newtonian Fluid Mech.*, 166 (2011), pp. 578–592.